Applied Physics Letters

Terahertz quantum cascade lasers based on type II InGaAs/GaAsSb/InP

Cite as: Appl. Phys. Lett. **97**, 261110 (2010); https://doi.org/10.1063/1.3532106
Submitted: 29 August 2010 • Accepted: 29 November 2010 • Published Online: 29 December 2010

Christoph Deutsch, Alexander Benz, Hermann Detz, et al.

Terahertz quantum cascade lasers based on type II InGaAs/GaAsSb/InP

Christoph Deutsch,[1,a)] Alexander Benz,[1] Hermann Detz,[2] Pavel Klang,[2] Michele Nobile,[2] Aaron Maxwell Andrews,[2] Werner Schrenk,[2] Tillmann Kubis,[3,4] Peter Vogl,[3] Gottfried Strasser,[2] and Karl Unterrainer[1]

[1]*Photonics Institute and Center for Micro- and Nanostructures, Technische Universität Wien, Gusshausstrasse 27-29, 1040 Vienna, Austria*

[2]*Institute for Solid State Electronics and Center for Micro- and Nanostructures, Technische Universität Wien, Floragasse 7, 1040 Vienna, Austria*

[3]*Walter Schottky Institute, Technische Universität München, Am Coulombwall 3, 85748 Garching, Germany*

[4]*Network for Computational Nanotechnology, Purdue University, 207 S Martin Jischke Drive, West Lafayette, Indiana 47906, USA*

(Received 29 August 2010; accepted 29 November 2010; published online 29 December 2010)

We report the demonstration of a terahertz quantum cascade laser based on the $In_{0.53}Ga_{0.47}As/GaAs_{0.51}Sb_{0.49}$ type II material system. The combination of low effective electron masses and a moderate conduction band offset makes this material system highly suitable for such devices. The active region is a three-well phonon depopulation design and laser ridges have been processed in a double-metal waveguide configuration. The devices exhibit a threshold current density of 2 kA/cm^2, provide peak optical powers of 1.8 mW, and operate up to 102 K. Emission frequencies are in the range between 3.6 and 4.2 THz. © *2010 American Institute of Physics*. [doi:10.1063/1.3532106]

Quantum cascade lasers[1] (QCLs) are promising sources in the terahertz range, but their convenient use in applications, such as imaging[2] or spectroscopy,[3] is hampered by the temperature performance of such devices.[4] Demonstrated in 2002,[5] a rapid development has pushed operating temperatures far beyond liquid nitrogen.[6] The last 5 years though only have brought an improvement of 22 K and operating temperatures are still not accessible by thermoelectric coolers. The record temperature operation at 186 K (Ref. 7) has been achieved by an optimization of the traditionally used $GaAs/Al_{0.15}Ga_{0.85}As$ material system for terahertz QCLs. However, at present, room temperature operation does not seem within reach by further optimization. All facts up to now reinforce the impression that future research should more and more focus on different concepts such as additional confinement[8] or other material systems with more favorable material properties.[4] For instance, in quantum dots, intersubband lifetimes of nanoseconds have recently been reported for terahertz transition energies.[9] In terms of the employed material system, a larger optical phonon energy, such as in GaN, would be highly desirable. In the midinfrared spectral range, the InP-based InGaAs/InAlAs material system with its low effective InGaAs electron mass and high conduction band offset is the key for high performance QCLs, emitting watts of light at room temperature.[10,11] Hence, early attempts have been made to transfer existing GaAs/AlGaAs active region concepts for terahertz QCLs to this low effective mass material system.[12] However, devices showed poor performance and subsequent improvement in design, growth, and processing could not close the gap to their GaAs-based predecessors.[13] Despite the lower effective electron mass, the high conduction band offset of 520 meV seems to compensate this advantage because it requires subnanometer barriers for engineering terahertz QCL active regions and consequently makes it very sensitive to growth variations. Therefore, the GaAs/AlGaAs material system is still the better choice for terahertz QCLs due to the flexibility in barrier heights provided by the inherent lattice matching conditions and excellent growth quality with low background doping densities.

Recently, optoelectronic intersubband devices based on the $In_{0.53}Ga_{0.47}As/GaAs_{0.51}Sb_{0.49}$ type II material system have been demonstrated including an Al-free midinfrared quantum cascade laser,[14] and quantum well infrared detectors.[15] The material parameters[16] are indeed genuinely attractive for terahertz QCLs: a lower conduction band offset (compared to InAlAs barriers) of 360 meV, extracted from intersubband absorption measurements, and low effective electron masses, which are $0.043m_0$ and $0.045m_0$ for the InGaAs wells and GaAsSb barriers, respectively. Key parameters for terahertz QCL active regions, such as the dipole matrix element of the radiative transition as well as the upper state lifetime, benefit from these low effective electron masses.[17] Larger dipole matrix elements directly translate into optical gain and decreased longitudinal optical (LO) phonon scattering rates result in an enhanced upper state lifetime, giving the prospect of higher temperature operation. The clear advantage for terahertz QCLs though is the moderate conduction band offset and the low effective electron barrier mass, which allows for thicker barriers in the active region. Consequently, the designed heterostructure becomes less sensitive to growth imperfections than the previously employed InGaAs/InAlAs material system. In addition, the effective electron barrier mass is further reduced by the nonparabolicity. Since the electrons tunnel deep in the quantum wells and the band structure alignment is of type II, the valence band influence on the effective mass is quite significant.[18] In fact, this causes a decreasing effective mass for decreasing energies, which makes tunneling more effective for lower energies.

We have engineered a three-well[19] $In_{0.53}Ga_{0.47}As/GaAs_{0.51}Sb_{0.49}$ active region for terahertz emission with a

a)Electronic mail: christoph.deutsch@tuwien.ac.at.

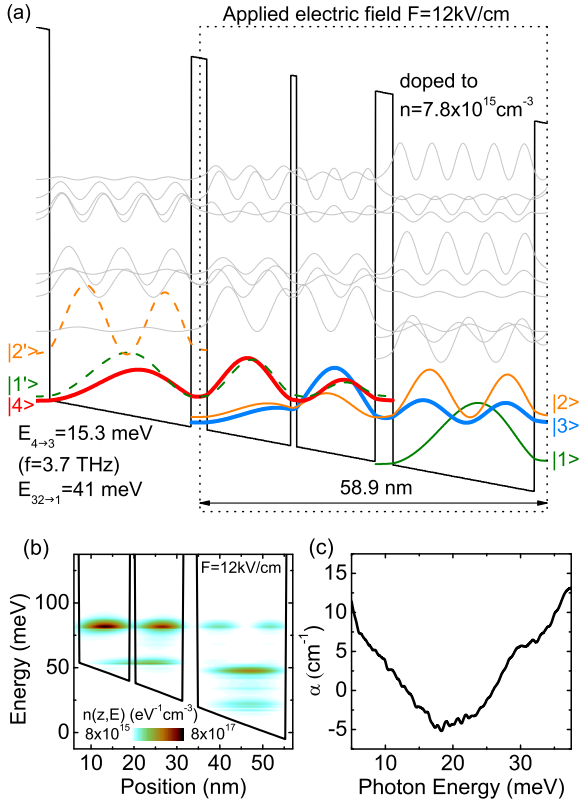

FIG. 1. (Color online) (a) Conduction band diagram of the three-well structure using a one-dimensional Schrödinger solver at an operating bias of 12 kV/cm. The radiative transition occurs from $|4\rangle \rightarrow |3\rangle$ (E_{43}=15.3 meV, f =3.7 THz). The energy gap for resonant depletion ($E_{32\rightarrow 1}$=41 meV) is slightly larger than the bulk $In_{0.53}Ga_{0.47}As$ LO phonon energy of 34 meV. The layer sequence in nanometer, starting from the injection barrier, is **2.4**/12.5/**0.9**/11.7/**2.6**/21.0 with the barriers indicated in bold fonts. The underlined 21.0 nm well is homogeneously doped to $n=7.8\times10^{15}$ cm^{-3}. (b) Contour plot of the energy resolved electron density in one module and (c) absorption/gain amplitude calculated with an NEGF transport code.

one-dimensional Schrödinger solver. Figure 1(a) displays the conduction band diagram at an applied electric field of 12 kV/cm. The optical transition between $|4\rangle$ and $|3\rangle$ has been designed to be 15.3 meV. Anticrossing energies of 4 meV for the injection and 5 meV for extraction path have been realized. The energy difference between the excited and the ground state in the widest well has been designed to be a few meV larger than the LO phonon energy in InGaAs (34 meV), which guarantees an efficient depopulation due to fast electron LO phonon scattering.[20] A homogeneous doping of $n=7.8\times10^{15}$ cm^{-3} in this well gives a two-dimensional carrier concentration of 1.6×10^{10} cm^{-2} per module. Furthermore, we have performed transport simulations based on nonequilibrium Green's function (NEGF) theory,[21] using the same material parameters as for the Schrödinger solver. The interface roughness has been assumed to be in the order of ±1 monolayer, which corresponds to a step height value of $\delta z=0.6$ nm, and with a typical correlation length of 8 nm.[21] Figure 1(b) illustrates the population inversion in the active region and the gain/absorption curve is displayed in Fig. 1(c), revealing a peak amplitude gain of 5.1 cm^{-1} at 18.1 meV. The slight discrepancy to the Schrödinger solver is caused by the adaptation of the barrier height to a coarser grid spacing for a reasonable computing time. The designed heterostructure was grown by solid-source molecular beam epitaxy[15] and consists of 170 periods with contact layers

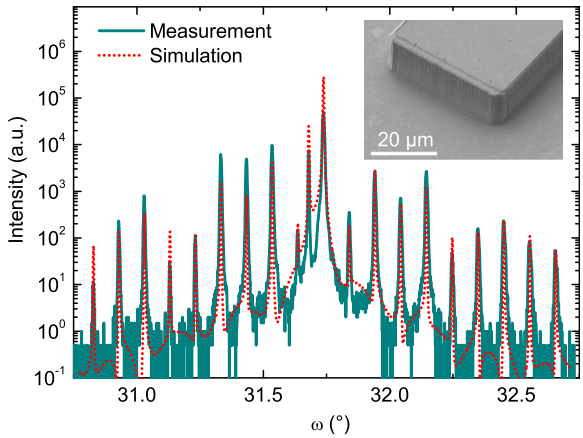

FIG. 2. (Color online) X-ray (004) rocking curve of the laser before processing. The inset shows a close-up of a facet, indicating the good quality of the dry-etched sidewalls.

doped to $n=7.2\times10^{18}$ cm^{-3} above (50 nm) and underneath (100 nm) the 9 μm thick active region. X-ray diffraction measurements performed before processing, shown in Fig. 2, confirmed the lattice-matched growth conditions and the unit cell period of 58.9 nm.

The active region was processed in a double-metal configuration since such a waveguide provides a modal overlap factor with the active region of almost unity, reasonably low losses, and high facet reflectivity. Ti/Au (10/1000 nm) bonding layers were deposited on the device wafer and a GaAs n+ receptor wafer, followed by a thermocompression wafer bonding step at 330 °C for 30 min under a constant pressure of 70 bars. Subsequently, the device substrate (InP) was removed by a combination of lapping and selective wet etching. Fabrication continued with standard lithography, defining the top metal layer, and a Ti/Au (10/800 nm) metallization. Final etching was performed in a reactive ion etching system using a $SiCl_4$:Ar environment and a 700 nm silicon nitride mask was used as a protection for the top metallization. In contrast to the majority of other reported double-metal terahertz QCL fabrication techniques both facets were also defined by lithography and dry-etching. The inset in Fig. 2 shows the high quality of the facets in such processed devices.

Devices were indium soldered on copper sample carriers, wire bonded, and mounted on a temperature controlled cold finger of a liquid helium flow cryostat equipped with a wedged TPX (polymethylpentene) window. The terahertz radiation was collected with an off-axis parabolic mirror detected with a liquid helium cooled silicon bolometer and measured with a lock-in amplifier. For absolute power values an Ophir 3A-SH thermopile power meter was used to calibrate the bolometer signal. The device was operated in pulsed mode with 300 ns long pulses at a repetition rate of 1.03 kHz for voltage versus current (IV) and light versus current (LI) characteristics. Spectra were recorded with a Bruker Vertex 80 Fourier transform infrared spectrometer with a resolution of 0.075 cm^{-1} and with an increased repetition rate of 10 kHz. Figure 3 displays the LIV characteristic of 1 mm long and 40 μm wide ridge device. At 8 K the threshold current density is 2 kA/cm^2 and the peak optical output power is 1.8 mW (not corrected for collection efficiency). This output power is a promising value compared to GaAs-based terahertz QCLs with similar pumping areas and

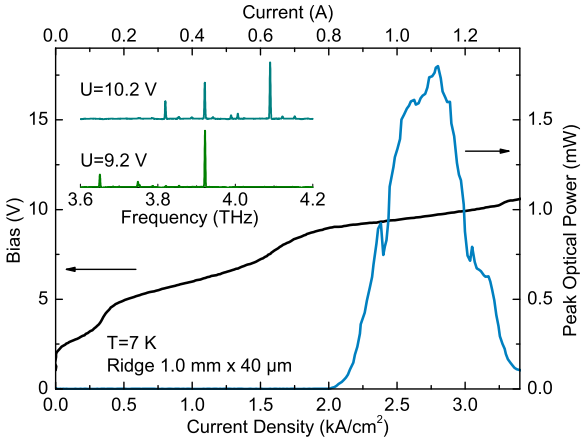

FIG. 3. (Color online) Pulsed (300 ns, 1.03 kHz) optical power and voltage vs current density characteristics of a ridge laser at a heat-sink temperature of 7 K. The inset shows two representative spectra.

facet dimensions. The spectra of the device are presented in the inset of Fig. 3 and show multiple modes between 3.6 and 4.2 THz, which is in good agreement with the calculated optical transition energy of 15.3 meV (f=3.7 THz) in the band structure simulation and also confirms the validity of the used parameters for the $In_{0.53}Ga_{0.47}As/GaAs_{0.51}Sb_{0.49}$ material system. The observed blue-shift at higher bias points and the relatively broad spectral range of lasing modes (≈0.6 THz) are likely to originate from the diagonal optical transition. This broad gain is also predicted by the NEGF simulation [see Fig. 1(c)]. Figure 4 displays the temperature dependence. The device shows lasing up to a heat-sink temperature of 102 K and the phenomenological expression $J_0+J_1\exp(T/T_0)$ for fitting J_{th} revealed a value of 24 K for T_0.

The measured threshold current density for this structure is quite high; however, it has to be mentioned that this initial design already showed lasing. The high threshold current could be due to a too high doping concentration or a slightly

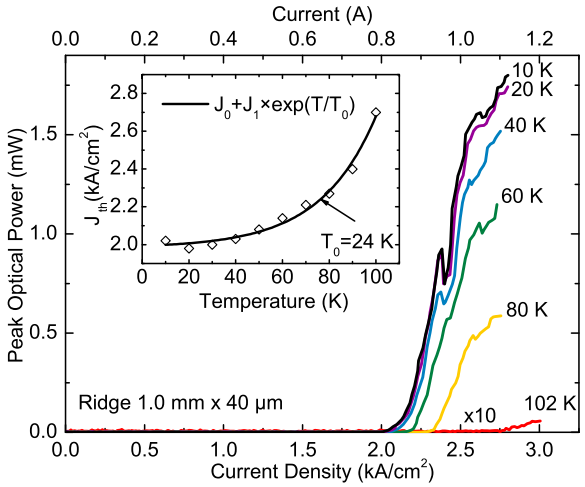

FIG. 4. (Color online) Peak optical power vs current density characteristics at various heat-sink temperatures emitted from a 1.0 mm long and 40 μm wide ridge waveguide. The device was operated under pulsed conditions (300 ns, 1.03 kHz). The inset illustrates the increased threshold current density at elevated temperatures and the commonly used phenomenological fit expression $J_{th}=J_0+J_1\exp(T/T_0)$ gives a value of 24 K for T_0.

imperfect design. The IV shows a pronounced kink below threshold at 5 V, which is attributed to the alignment of $|1'\rangle$ with $|2\rangle$. A revised design with lower anticrossing of these two states should decrease this current channel and hence decrease the threshold.[7]

In conclusion, we realized the first terahertz quantum cascade lasers in the $In_{0.53}Ga_{0.47}As/GaAs_{0.51}Sb_{0.49}$ type II material system emitting around 3.9 THz. A reasonable device performance up to a heat-sink temperature of 102 K and a peak optical power as high as 1.8 mW proves that this InP-based heterostructure with its low effective masses and moderate conduction band offset also has a lot of potential in the terahertz range. Next generation devices with lower thresholds through refined active region designs, better growth quality, and improved processing have a good prospect of being competitive to state-of-the-art $GaAs/Al_{0.15}Ga_{0.85}As$ terahertz QCLs.

The authors acknowledge the support by the Austrian Scientific Fund FWF (SFB-ADLIS, SFB-IRON, and DK Co-QuS), the Austrian Nano Initiative project (PLATON), and the Austrian Society for Microelectronics (GMe).

[1] J. Faist, F. Capasso, D. L. Sivco, C. Sirtori, A. L. Hutchinson, and A. Y. Cho, Science **264**, 553 (1994).
[2] J. Darmo, V. Tamosiunas, G. Fasching, J. Kröll, K. Unterrainer, M. Beck, M. Giovannini, J. Faist, C. Kremser, and P. Debbage, Opt. Express **12**, 1879 (2004).
[3] H.-W. Hübers, S. G. Pavlov, H. Richter, A. D. Semenov, L. Mahler, A. Tredicucci, H. E. Beere, and D. A. Ritchie, Appl. Phys. Lett. **89**, 061115 (2006).
[4] B. S. Williams, Nat. Photonics **1**, 517 (2007).
[5] R. Köhler, A. Tredicucci, F. Beltram, H. E. Beere, E. H. Linfield, A. G. Davies, D. A. Ritchie, R. C. Iotti, and F. Rossi, Nature (London) **417**, 156 (2002).
[6] B. S. Williams, S. Kumar, and Q. Hu, Opt. Express **13**, 3331 (2005).
[7] S. Kumar, Q. Hu, and J. L. Reno, Appl. Phys. Lett. **94**, 131105 (2009).
[8] A. Wade, G. Fedorov, D. Smirnov, S. Kumar, B. S. Williams, Q. Hu, and J. L. Reno, Nat. Photonics **3**, 41 (2009).
[9] E. A. Zibik, T. Grange, B. A. Carpenter, N. E. Porter, R. Ferreira, G. Bastard, D. Stehr, S. Winnerl, M. Helm, H. Y. Liu, M. S. Skolnick, and L. R. Wilson, Nature Mater. **8**, 803 (2009).
[10] Y. Bai, S. Slivken, S. R. Darvish, and M. Razeghi, Appl. Phys. Lett. **93**, 021103 (2008).
[11] A. Lyakh, C. Pflügl, L. Diehl, Q. J. Wang, F. Capasso, X. J. Wang, J. Y. Fan, T. Tanbun-Ek, R. Maulini, A. Tsekoun, R. Go, and C. K. N. Patel, Appl. Phys. Lett. **92**, 111110 (2008).
[12] L. Ajili, G. Scalari, N. Hoyler, M. Giovannini, and J. Faist, Appl. Phys. Lett. **87**, 141107 (2005).
[13] M. Fischer, G. Scalari, Ch. Walther, and J. Faist, J. Cryst. Growth **311**, 1939 (2009).
[14] M. Nobile, P. Klang, E. Mujagić, H. Detz, A. M. Andrews, W. Schrenk, and G. Strasser, Electron. Lett. **45**, 1031 (2009).
[15] H. Detz, A. M. Andrews, M. Nobile, P. Klang, E. Mujagić, G. Hesser, W. Schrenk, F. Schäffler, and G. Strasser, J. Vac. Sci. Technol. B **28**, C3G19 (2010).
[16] M. Nobile, H. Detz, E. Mujagić, A. M. Andrews, P. Klang, W. Schrenk, and G. Strasser, Appl. Phys. Lett. **95**, 041102 (2009).
[17] E. Benveniste, A. Vasanelli, A. Delteil, J. Devenson, R. Teissier, A. Baranov, A. M. Andrews, G. Strasser, I. Sagnes, and C. Sirtori, Appl. Phys. Lett. **93**, 131108 (2008).
[18] J. R. Söderström, E. R. Brown, C. D. Parker, L. J. Mahoney, J. Y. Yao, T. G. Andersson, and T. C. McGill, Appl. Phys. Lett. **58**, 3 (1991).
[19] H. Luo, S. R. Laframboise, Z. R. Wasilewski, G. C. Aers, J. C. Cao, and H. C. Liu, Appl. Phys. Lett. **90**, 041112 (2007).
[20] B. S. Williams, H. Callebaut, S. Kumar, Q. Hu, and J. L. Reno, Appl. Phys. Lett. **82**, 1015 (2003).
[21] T. Kubis, C. Yeh, P. Vogl, A. Benz, G. Fasching, and C. Deutsch, Phys. Rev. B **79**, 195323 (2009).